Full-Field Quantum Correlations of Spatially Entangled Photons

V. D. Salakhutdinov, E. R. Eliel, and W. Löffler*

Huygens Laboratory, Leiden University, P.O. Box 9504, 2300 RA Leiden, The Netherlands
(Received 5 November 2011; published 23 April 2012)

Spatially entangled twin photons allow the study of high-dimensional entanglement, and the Laguerre-Gauss modes are the most commonly used basis to discretize the single-photon mode spaces. In this basis, to date only the azimuthal degree of freedom has been investigated experimentally due to its fundamental and experimental simplicity. We show that the full spatial entanglement is indeed accessible experimentally; i.e., we have found practicable radial detection modes with negligible cross correlations. This allows us to demonstrate hybrid azimuthal-radial quantum correlations in a Hilbert space with more than 100 dimensions per photon.

High-dimensional entangled photons are of great interest in various areas in quantum information, as they promise high-density encoding of quantum information [1,2], are more robust against noise and eavesdroppers due to stronger nonclassical correlations [3], and, in general, present a unique model system for the study of high-dimensional entanglement in nature. Entanglement in the photon's spatial degrees of freedom is a candidate for this, and it can readily be obtained in the laboratory by spontaneous parametric down-conversion (SPDC) of an intense laser beam. To explore this high-dimensional Hilbert space, we need to discretize this initially continuous space; due to the paraxial nature of experiments, this is usually done by using a complete and orthogonal basis of transverse optical modes. In quantum information with entangled particles, it is crucial that the bipartite state shows perfect correlation (or anticorrelation) in the used quantum numbers. Paraxial optical modes are also required for the implementation of quantum cryptography: They are propagation-invariant, and superpositions thereof are basically stable. Traditionally, a Gaussian basis is employed; in particular, the Laguerre-Gaussian modes LG_p^ℓ with mode indices ℓ and p proved to be very convenient. These modes factor in an azimuthal phase-only part $u_{az}^\ell(\phi) = e^{i\ell\phi}$ and a radial part $u_{rad}^{p,\ell}(r)$, in which the azimuthal part gives rise to the photon orbital angular momentum (OAM) of $\ell\hbar$ [4]. This azimuthal part, or OAM entanglement, has been subject to a decade of numerous very successful experiments (see, e.g., Refs. [5,6]), which is well founded by the fact that most experimental setups exhibit rotation symmetry around the optical axis.

The amount of entanglement present in the spatial photon pairs can be characterized by the *average* number of entangled optical modes, the Schmidt number K [7,8]. This Schmidt number $K = 1/\sum_k \lambda_k^2$ is obtained from the eigenvalues (relative weights) λ_k of the Schmidt decomposition [9] of the two-photon field $|\Psi\rangle = \sum_k \sqrt{\lambda_k} |u_k\rangle_s |u_k\rangle_i$, where the $|u_k\rangle_{s,i}$ are the Schmidt eigenmodes for the signal or idler photon. Although the Schmidt modes have to be

calculated numerically in the general case, the Schmidt number K can be approximated as $K = \frac{1}{4}(b\sigma + \frac{1}{b\sigma})^2$, where b^{-1} (with $b^2 = L\lambda_p/8\pi$) is the phase-matching width and σ is the pump-beam waist [7]. For our experimental parameters (crystal length $L = 2$ mm, pump-beam waist $w_p = 325$ μm, pump-beam wavelength $\lambda_p = 413$ nm), this number is very large: $K \approx 350$. However, if only the azimuthal degree of freedom is employed (i.e., by taking $p = 0$ [10]), this number is significantly lower. We can write the two-photon entangled state as $|\psi\rangle = \sum_{\ell=-\infty}^{+\infty} \sqrt{\lambda_\ell} |\ell, p = 0\rangle_s |-\ell, p = 0\rangle_i$, where $|\ell, p\rangle$ is a photon with OAM $\ell\hbar$ and radial quantum number p, and the (azimuthal) Schmidt number becomes $K_{az} = 1/\sum_\ell \lambda_\ell^2$. For large K, this can be approximated as $K_{az} \approx 2\sqrt{K}$ [11,12]. Direct experimental determination of this number has been shown only recently [13]. For our case, this number is $K_{az} \approx 37$, which is obviously much lower than the total number of entangled modes. The "missing" entanglement becomes accessible if also the radial modes are taken into account. There, we find a *radial* Schmidt number (for only one azimuthal mode, e.g., for $\ell = 0$) $K_{rad} \approx \sqrt{K}$, which in our example is $K_{rad} \approx 18$. The vast majority of the entangled modes are radial-azimuthal cross-correlated modes [14].

Subject to experimental feasibility, the radial part of the Laguerre-Gauss entangled modes is an entanglement resource on equal footing; however, only recently has it been investigated in detail theoretically [15]. The LG mode functions factor as $\mathrm{LG}_p^\ell(r, \phi) = Cu_{az}^\ell(\phi)u_{rad}^{p,\ell}(r)$; the azimuthal part is fully orthogonal in ℓ and independent on the experimental choice of the detection-mode waist, and the entangled photons are perfectly anticorrelated in ℓ: OAM is conserved in SPDC (in Fig. S1 of Ref. [16], we show that this statement holds also for higher-order radial modes). Therefore, the azimuthal modes are automatically Schmidt modes. It turns out that, in contrast to this, the radial modes do not necessarily represent Schmidt modes [7], and we expect to find nonzero quantum correlations of detected
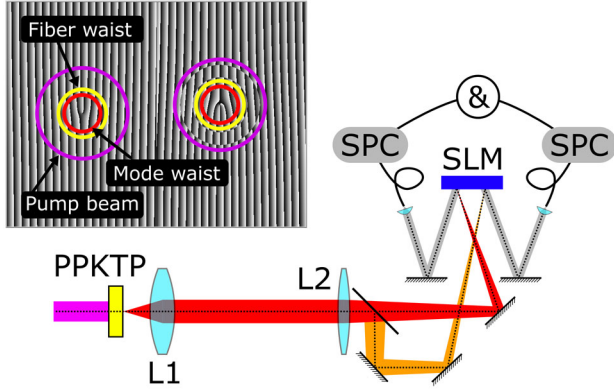
FIG. 1 (color online). Schematic experimental setup. The spatially entangled photons are produced in the nonlinear crystal, whose surface is imaged with 7.5× magnification ($f_{L1} = 10$ cm, $f_{L2} = 75$ cm) onto the spatial light modulator (display size 16×12 mm², 800×600 pixel). This device is programmed to perform the phase modulation required to transform the detection mode into the fundamental mode. The far field of the SLM surface is imaged ($10\times$, 0.2 numerical aperture objectives) onto the single-mode fiber which is connected to a single-photon counter. Simultaneous detection events from an entangled photon pair are selected in a coincidence time window of 2.3 ns. The inset shows an exemplary SLM phase pattern ($\ell_s = 1$, $p_s = 1$; $\ell_i = -2$, $p_i = 3$) and superimposed the magnification-corrected waist of the pump beam (purple), the waist of the detection single-mode fiber (1275 mm, yellow), and the detection-mode waist (red) $w = 1000$ μm.

modes with different p. However, for a proper combination of pump-beam, detection-mode, and phase-matching waist $w^*_{s,i} = \sqrt{4b/\sigma}$ [7,11], also the radial LG modes are Schmidt modes and the cross correlations for $p_s \neq p_i$ disappear. In our case, we obtain $w^*_{s,i} = 37$ μm. If we neglect phase matching [15], $w^*_{s,i} \rightarrow 0$.

Also experimentally, investigation of the radial correlations turns out to be more challenging: The spatial correlations are traditionally investigated by using a mode converter (spatial light modulator or spiral phase plate in the case of azimuthal correlations), to transform a certain optical mode into the fundamental Gaussian, which in turn can be tested by sending the photon into a single-mode fiber. This works very well for the azimuthal modes, but for radial modes, complications occur: For instance, the finite acceptance angle of the single-mode fiber becomes problematic, and there are no perfect spatial modulators which allow control over amplitude *and* phase simultaneously (the orthogonality of p modes requires amplitude-sensitive detection), and careful choices for the detection-mode waist and the fiber collimator have to be taken [7]. We show here that, despite these complications, and under the right conditions, the relation between the analyzer modes and the pump field becomes nicely visible, and a properly correlated mode basis can be obtained.

Experiment.—We generate the spatially entangled photon pairs by collinear SPDC in a periodically poled

KTiOPO₄ (PPKTP) crystal (length $L = 2$ mm) of a LG_0^0 laser beam (Kr⁺, $\lambda = 413$ nm, beam waist at crystal $w_p = 325$ μm, 50 mW power).

As sketched in Fig. 1, we image the crystal surface with 7.5× magnification using a telescope onto the spatial light modulator (SLM) surface. The SLM is used under an incident angle of 10° or 5°; this allows us to use a single SLM for both the signal and idler photon. The SLM is corrected for phase flatness, and we operate not in direct phase modulation but use a blaze towards 2 mrad to further lessen the influence of phase errors. The far field of the SLM surface is imaged onto the single-mode fiber using 10× objectives, with a detection-fiber mode waist at the SLM of 1275 μm. The fibers are connected to single-photon counters, and we postselect entangled photon pairs by coincidence detection (time window 2.3 ns). Since the crystal surface is *imaged* onto the SLM, it is sufficient to discuss the situation there. The inset in Fig. 1 shows the resulting waists of the pump beam, the detection mode, and the detection single-mode fiber, with exemplary phase patterns for two different settings of the detection-mode quantum numbers. The choice of waists depends on (i) the desired ratio $\gamma = w_p/w_{s,i}$, which determines the orthogonality and overlap with the Schmidt modes (where the ideal ratio is $\gamma^* = 8.8$), (ii) the maximum mode order which should be detected—this is connected to the single-mode detection-fiber mode waist—and (iii) the number of entangled modes required. Our choice of waists is optimized for radial and azimuthal mode numbers up to about 10.

Our SLM-based mode detectors cannot project upon perfect LG modes, because the amplitude cannot be modulated (this is not possible with conventional SLMs [17]). This can lead to p-nonorthogonal detection fields u_p^ℓ because $\int_0^\infty \arg[LG_{p_1}^\ell(r)LG_{p_2}^\ell(r)] \neq \delta_{p_1,p_2}$, and one would anticipate that cross correlations will always appear; our results below show that this is not always true and that careful adjustment of the detection-mode waist allows detection of radially entangled modes with negligible cross correlations. Basically, optical diffraction couples phase and amplitude, which helps to obtain amplitude-sensitive detection.

For theoretical calculation of the expected coincidence count rate, we apply Klyshko's picture of advanced waves [18]. The detection field (in the near field of the SLM) is determined by the Gaussian amplitude of the single-mode detection fiber and the phase as defined by the SLM: $u_{xtal}^{p,\ell} = \exp\{i \arg[LG_p^\ell] - r^2/w_{SMF}^2\}$. We then decompose this field in terms of LG modes: $u_{xtal}^{p,\ell} = \sum_{p'} \alpha_{p',\ell} LG_{p'}^\ell$. This expansion contains very high-order p components due to the phase jumps at the zeros of the LG polynomial with finite intensity. These singularities automatically disappear while weighting the modes with their relative weight as produced in SPDC $C_{p,p}^{\ell,-\ell}$ [Eq. (20) in Ref. [15]]. This results in $\alpha'_{p',\ell} = 2\pi\sqrt{C_{p',p'}^{\ell,-\ell}} \int dr r LG_{p'}^\ell(r) u_{xtal}^{p,\ell}$, which

allows us to calculate the effective detection field at the crystal $u_{\mathrm{det}}^{p,\ell} = \sum_{p'} \alpha_{p',\ell} \mathrm{LG}_{p'}^{\ell}$. To obtain the coincidence amplitude, we can then simply calculate the overlap of the two individual detection fields in the signal and idler path: $C' = \int d^2 r u_{\mathrm{det}}^{p_s,\ell_s} u_{\mathrm{det}}^{p_i,\ell_i}$. Finally, the experimentally observable coincidence count rate is $\Gamma = |C'|^2$. We use here the thin-crystal limit $(L \to 0)$, which implies that phase-matching effects are neglected (experimentally, we are close to perfect phase matching).

Radial-mode correlations.—Figure 2 shows the quantum correlations of purely radial modes $(\ell_s = \ell_i = 0)$ of down-converted photons. We clearly observe, as we decrease the detection-mode waist, that the off-diagonal elements in the correlation matrix decrease. This is expected; as mentioned above, the radial cross correlations disappear for $w_{s,i} \to w_{s,i}^*$. To within our experimental accuracy, we

also reproduce the theoretical results of Miatto, Yao, and Barnett [15] very well. Even minute details of the experimental data are reproduced qualitatively well by our model (Fig. 2); this suggests that our modeling approach of expanding the detection field in terms of the LG modes provided by the SPDC light is a sound choice. For the case of a 500 μm mode waist, we estimate the (radial) Schmidt number to be 10.4 (experiment) and 11.2 (theory). This is less than the expectation mentioned above ($K_{\mathrm{rad}} = 18$); however, SLM pixilation becomes relevant at such small mode waists. To investigate this, we determine a measure of the cross correlations, or the width of the diagonal (Fig. 2) around $p_s = p_i$: $W = \sum_p \Gamma(p_s = p_i = p) / \sum_{p_s,p_i} \Gamma(p_s, p_i)$. For perfectly orthogonal modes, W should be unity. Figure 3 shows W as a function of the beam waist, comparing our theoretical simulation with experimental data; again we find good agreement. This dependency of the cross correlations on the beam waist ratio persists also for higher azimuthal modes ($\ell_s = -\ell_i$), as shown in Fig. S2 of Ref. [16]. We observe that for a detection-mode waist smaller than 500 μm, the "orthogonality" W decreases again; this (and the fact that the theoretical curve does not reach unity) is a consequence of SLM pixilation: A 500 μm waist corresponds to ~25 pixel of the SLM. Our results also demonstrate that the apprehension of Miatto, Yao, and Barnett [15], that the experimentally accessible mode waist ratios γ are too small, therefore leading to strong cross correlation in p space, which would
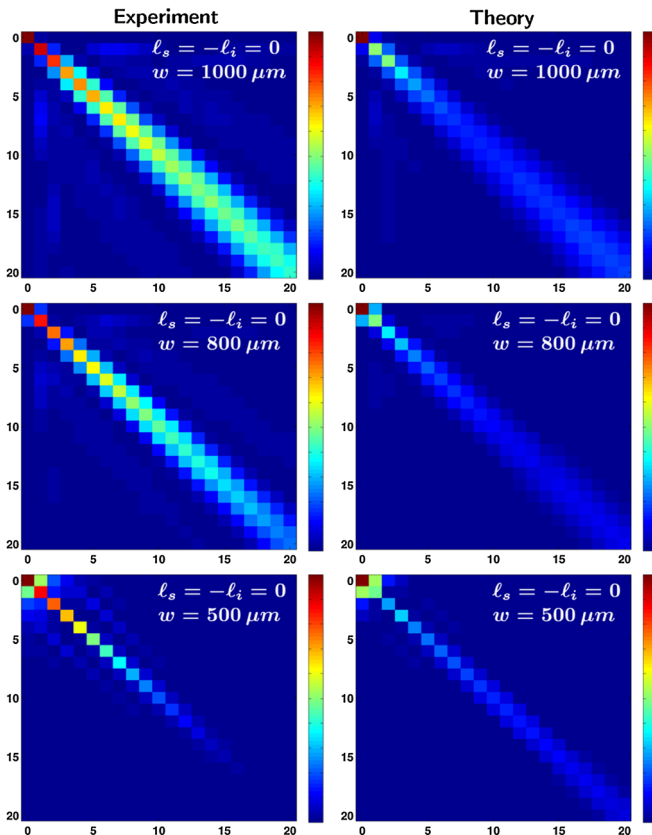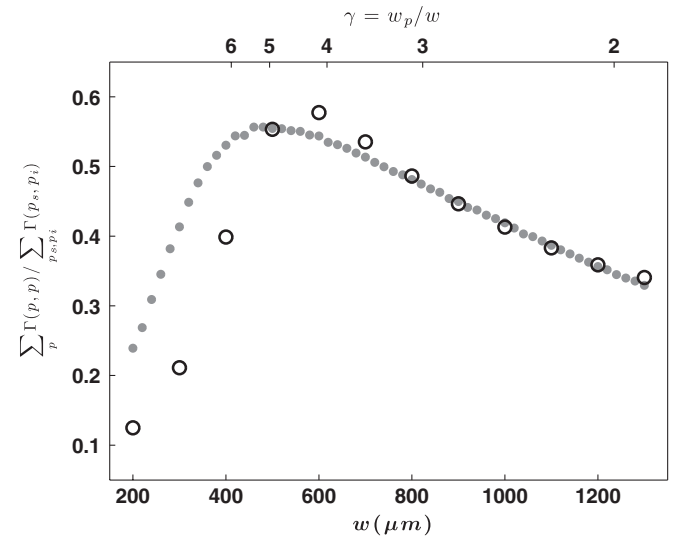

FIG. 2 (color online). Quantum correlations between radial modes with different p (for $\ell_s = \ell_i = 0$): Shown are the normalized (divided by maximum) coincidence count rates (color coded) as a function of the radial-mode numbers p_s (horizontal axis) and p_i (vertical axis) of the detection modes. Different rows depict results for different detection-mode waists as indicated. Left column, experimental data; right column: theoretical prediction. It is clearly visible that the smaller the detection-mode waist gets, the smaller the off-diagonal counts will be. This is a sign that we approach the Schmidt basis for $\gamma \to \gamma^*$. The detection-mode waists corresponds to waist ratios of (from top to bottom) $\gamma = 2.4, 3, 4.9$; see [15].

FIG. 3. The influence of the detection-mode waist: The quantity on the y axis is a measure of how sharply the radial quantum correlations peak around $p_s = p_i$. For ideal LG mode detectors, we have $W \to 1$ for the waist ratio $\gamma \to \gamma^*$. For small waists ($w < 500$ μm), pixilation effects are non-negligible. For larger waists, the agreement between experiment (circles) and theory (gray dots) is very good. The top axis indicates the ratio γ of the pump-beam waist w_p to the detection-mode waist $w = w_{s,i}$ of the signal and idler photon.
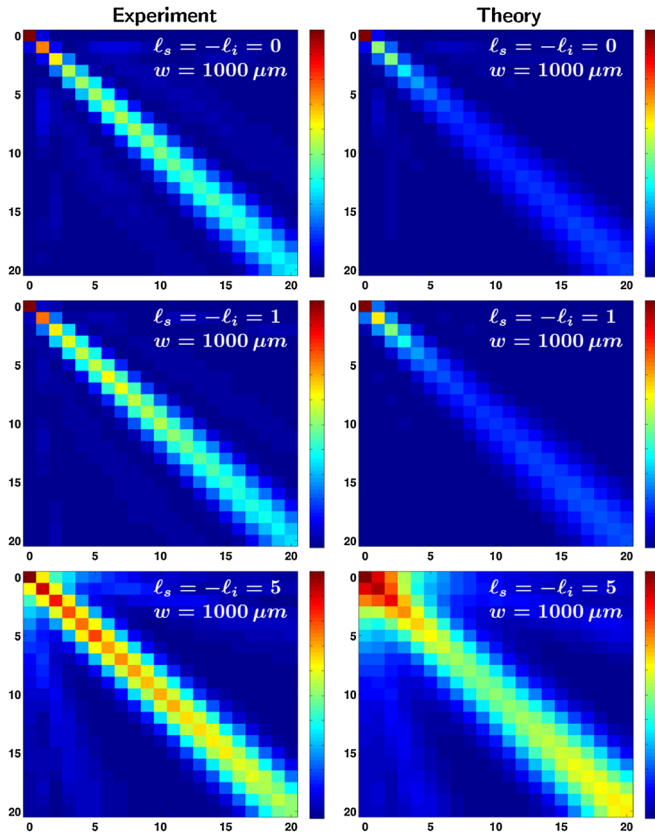
FIG. 4 (color online). Quantum correlations between radial modes with different p, for given ℓ (rows) at a fixed waist ratio $\gamma = 2.4$. The left column shows experimental data, the right column the theoretical prediction. The number of single-particle modes involved in these experiments is approximately 100.

imply that radial modes are not useful for quantum information, is overcautious: We can adjust the mode waists so that cross correlations become negligible.

Radial-azimuthal correlations.—Finally, we address the question of whether we can make use of the full azimuthal-radial Hilbert space *experimentally*. We find that, independent on the radial-mode index p, the anticorrelation condition $\ell_s = -\ell_i$, or OAM conservation, is preserved for high values (up to ≈ 20) of p and ℓ (see Fig. S1). Figure 4 shows p correlations for a fixed detection-mode waist of 1000 μm, as in Fig. 2, but this time for different choices of $\ell_s = -\ell_i \equiv \ell$. Compared to $\ell = 0$, we observe a negligible increase of the cross correlations for $p_s \neq p_i$, which is very encouraging, because this suggests that very high-dimensional Hilbert spaces become accessible. Additionally, the $p_s = p_i$ correlations get more evenly distributed, in agreement with theoretical predictions [15], which also increases the number of usable modes. Our results in Fig. 4 show two-photon correlations in an approximately 100×100-dimensional Hilbert space.

Conclusions.—In conclusion, we have shown the first experiments with high-dimensionally spatially entangled photons in the full Laguerre-Gauss-like basis. We analyze the entangled photons in the complete transverse basis involving azimuthal and radial correlations; this goes a step forward beyond the conventionally used azimuthal degree of freedom, or orbital angular momentum entanglement. We find that the radial degree of freedom is indeed a useful entanglement resource, if care is taken: Our experiments and the theoretical model show that the choice of detection-mode waist is crucial and has to be taken into account carefully; we are able to demonstrate the transition to a detection basis where cross correlations disappear, effectively a transition to a quasi-Schmidt basis. An important next step will be confirmation and quantification of the "hybrid" azimuthal-radial-mode entanglement, which is beyond the scope of this Letter. If radial modes in spatial entanglement are accessible, the number of useful entangled modes is roughly squared compared to the OAM case; this quadratic increase in the usable Schmidt number could stimulate new experiments like detection-loophole-free [19] Bell tests. The higher entanglement density per mode area will also enable higher channel capacities in systems where the spatial extent is relevant: for the transport of spatially entangled photons through optical fibers [20] and also through turbulent atmosphere [21].

*loeffler@physics.leidenuniv.nl

[1] C. H. Bennett and S. J. Wiesner, Phys. Rev. Lett. **69,** 2881 (1992).
[2] H. Bechmann-Pasquinucci and W. Tittel, Phys. Rev. A **61,** 062308 (2000).
[3] D. Kaszlikowski, P. Gnaciński, M. Żukowski, W. Miklaszewski, and A. Zeilinger, Phys. Rev. Lett. **85,** 4418 (2000).
[4] L. Allen, M. W. Beijersbergen, R. J. C. Spreeuw, and J. P. Woerdman, Phys. Rev. A **45,** 8185 (1992).
[5] A. Mair, A. Vaziri, G. Weihs, and A. Zeilinger, Nature (London) **412,** 313 (2001).
[6] A. C. Dada, J. Leach, G. S. Buller, M. J. Padgett, and E. Andersson, Nature Phys. **7,** 677 (2011).
[7] C. K. Law and J. H. Eberly, Phys. Rev. Lett. **92,** 127903 (2004).
[8] J. P. Torres, A. Alexandrescu, and L. Torner, Phys. Rev. A **68,** 050301 (2003).
[9] A. Ekert and P. L. Knight, Am. J. Phys. **63,** 415 (1995).
[10] C. I. Osorio, G. Molina-Terriza, and J. P. Torres, Phys. Rev. A **77,** 015810 (2008).
[11] M. P. van Exter, A. Aiello, S. S. R. Oemrawsingh, G. Nienhuis, and J. P. Woerdman, Phys. Rev. A **74,** 012309 (2006).
[12] M. P. van Exter, P. S. K. Lee, S. Doesburg, and J. P. Woerdman, Opt. Express **15,** 6431 (2007).

[13] H. Di Lorenzo Pires, H. C. B. Florijn, and M. P. van Exter, Phys. Rev. Lett. **104**, 020505 (2010).

[14] S. S. Straupe, D. P. Ivanov, A. A. Kalinkin, I. B. Bobrov, and S. P. Kulik, Phys. Rev. A **83**, 060302 (2011).

[15] F. M. Miatto, A. M. Yao, and S. M. Barnett, Phys. Rev. A **83**, 033816 (2011).

[16] See Supplemental Material at http://link.aps.org/supplemental/10.1103/PhysRevLett.108.173604 for additional experimental data on OAM correlations with $p \neq 0$ and on p-dependent cross correlations for $\ell \neq 0$.

[17] Amplitude-shaped holograms (as used in, e.g., [6]) are not suitable for small-angle holograms like the ones used here; they do not produce phase-correct fields in the far field of the first diffraction order.

[18] D. Klyshko, Phys. Lett. A **132**, 299 (1988).

[19] T. Vértesi, S. Pironio, and N. Brunner, Phys. Rev. Lett. **104**, 060401 (2010).

[20] W. Löffler, T. G. Euser, E. R. Eliel, M. Scharrer, P. S. J. Russell, and J. P. Woerdman, Phys. Rev. Lett. **106**, 240505 (2011).

[21] B.-J. Pors, C. H. Monken, E. R. Eliel, and J. P. Woerdman, Opt. Express **19**, 6671 (2011).